Research Square

Preprints are preliminary reports that have not undergone peer review.
They should not be considered conclusive, used to inform clinical practice,
or referenced by the media as validated information.

Protein Partitioning In A Droplet-Based Aqueous-Two Phase System Microfluidic Device

David Hernández Cid
Tecnologico de Monterry, Campus Monterrey
Roberto Carlos Gallo-Villanueva
Tecnologico de Monterry, Campus Monterrey
José González-Valdez
Tecnologico de Monterry, Campus Monterrey
Victor Hugo Pérez González
Tecnologico de Monterry, Campus Monterrey
Marco Arnulfo Mata-Gómez (mmatag@tec.mx)
Tecnologico de Monterry, Campus Monterrey

Research Article

Keywords: Systems, phase, microfluidic, proteins

Posted Date: October 26th, 2021

DOI: https://doi.org/10.21203/rs.3.rs-967209/v1

License: This work is licensed under a Creative Commons Attribution 4.0 International License.
Read Full License

Protein partitioning in a droplet-based aqueous-two phase system microfluidic device

D. Hernández-Cid[a], R.C. Gallo-Villanueva[a], J. González-Valdez[a], V.H. Perez-Gonzalez[a,*], M.A. Mata-Gómez[*, a, b]

[a] *Tecnologico de Monterry, Campus Monterrey, School of Egineering and Science, Av. Eugenio Garza Sada 2501, Monterrey, N.L., México, 64849*

[b] *Tecnologico de Monterry, Campus Puebla, School of Egineering and Science, Vía Atlixcáyotl 5718, Reserva Territorial Atlixcáyotl, Puebla, Puebla, México, 72453*

***Corresponding authors:**

Marco A. Mata-Gómez, mmatag@tec.mx

Victor H. Perez-Gonzalez, vhpg@tec.mx

Keywords: microfluidics, droplets, Aqueous two-phases systems, bioseparation

Abstract

Aqueous-Two Phase Systems (ATPS) is an important tool for the separation of biological entities as proteins, membranes, enzymes, among others. On the other hand, microfluidics is an emerging technology that studies and manipulates liquids either one single phase or dispersed fluids such as droplets at the micro or smaller scales. Applications of microfluidics in different areas such as molecular biology, biochemical analysis and bioprocess have increased in the last years. In this work, we proposed a droplet-based microfluidic approach to generate ATPS systems and to observe how two model proteins, native ribonuclease A (RNase A) and its PEGylated form (PEG-RNase A), behave and partition on these systems. Using polyethylenglycol (PEG) and potasium phosphate salts as the phase-forming chemicals, we were able to form ATPS systems inside the microfluidic device as commonly performed in conventional ATPS macrosystems. Even more, formation of ATPS systems in which one of the fluids was present as a droplet was also achieved. As expected, model proteins exhibited the same behavior as they do in a macrosystem, that is, they displaced to a particular phase according to their affinity for them. When native RNase A was placed in the salt-rich phase, it remained there, and migrated from the PEG-rich phase to the former. On its part, PEGylated RNase A remained in the PEG-rich phase or migrated from salt-rich phase to the PEG-rich phase. These results open the possibility for a prospect of micro bioprocess to separate interest biomolecules.

1. Introduction

Aqueous-two phase system (ATPS) is a downstream processing technique used to fractionate proteins, and other small biomolecules, based on their affinity to one of the two phases. Systems are formed usually of a polymer, such as polyethylene glycol (PEG) or dextran, and a salt, but polymer-polymer, or even alcohol-salt systems, have also been explored (Asenjo & Andrews, 2011; Hatti-Kaul, 2001). Beyond the traditional use of ATPS, its implementation in microfluidic devices is a quite new and fertile field where important contributions have been made. Lu et al. [3] experimentally studied the stability of the parallel laminar flow regime of ATPS in microchannels (Lu et al., 2011). To do this, they used branched microchannels, and they were able to generate a map to identify different regimes (i.e., bi-laminate flow or droplets). Furthermore, Meagher et al. [4] demonstrated protein separation in ATPS via diffusion between streamlines, where PEG-rich and salt-rich phases were used. They used FITC to track proteins moving towards the PEG-rich phase. On another experiment they demonstrated the partitioning of bovine serum albumin and β-galactosidase between the two streams (Meagher et al., 2008).

Droplet based microfluidics is a subcategory of microfluidics dedicated to the generation of discrete volumes of one fluid dispersed in another fluid, both fluids being immiscible. Droplets can be used as microreactors for biochemical analysis or synthesis (Song et al., 2006; Taly et al., 2007). Recently, efforts have been made to generate droplets using the typical salt-polymer systems usually selected for ATPS formation in microfluidic devices (Hardt & Hahn, 2012). The idea is forming two phases, but one of them in a droplet-like shape, and the other remaining intact outside the boundary of the droplet (similarly to traditional systems). Theoretically, this would allow the encapsulation or separation of cells or other biomolecules. For instance, Moon et al. [8] presented a technique that generated droplets using ATPS. Their method consisted of a flow-focusing device with a precisely controlled pulsating inlet pressure. For this work they used dextran and PEG as the disperse and continuous phase, respectively. The use of on-off cycles, combined with the fixed flow rate cross-flow of the PEG phase, made it possible to generate droplets in the jetting regimen (Moon et al., 2015). Also, Zhou et al. (Zhou et al., 2017) presented an approach to produce uniform ATPS droplets facilitated by oil-droplet choppers. This method consists of the generation of high interfacial tension oil-in-water droplets and low interfacial tension water-in-water droplets, in which the interface of the ATPS is distorted by oil droplets and decays into water-in-water droplets. They demonstrated high droplet uniformity with a wide range of droplet sizes, and a maximum frequency of generation of about 2.1 kHz [9]. More recently, Mohammad et al. [10] presented, for the first time, the passive generation of salt based ATPS droplets. They tested polymer/polymer, and polymer/salts systems (i.e. PEG/dextran and PEG/Magnesium salts, respectively). In this work, they were able to encapsulate umbilical vein endothelial cells (HUVECs) in PEG/salt microdroplet systems, which is of high utility in biotechnological applications as cell sorting and drug discovery. To the best of our knowledge no work has encompassed the use of microfluidic droplet based ATPS made by polymers and salts for protein partitioning (Mastiani et al., 2019).

Here, we propose an ATPS droplet-based microfluidic device as a first approach to visualize the protein partitioning behavior. The idea behind this is to emulate the traditional PEG-salt ATPS by a droplet-shape phase and a flowing phase outside the droplet at a microscale level. Native ribonuclease A (RNase A) and its PEGylated form were used as protein models as their partition behavior in traditional ATPS systems has been well studied [8, 9]. While the former has affinity for the salt-rich phase, the latter has affinity for the PEG rich phase. So, it was hypothesized that both proteins would behave in the same manner inside the ATPS microdroplet generator i.e., remining at or partitioning towards the phase for which they have more affinity.

2. Theory

An aqueous two-phases system (ATPS) forms when the components (polymers-water-salt) exceed the solubility limits and generate new phases. A graphic to represent the solubility is the binodal curve (Fig. 1). Above the curve, we found the biphasic systems, and under the curve the monobasic systems. The total concentration of each component of the system is given by the values of x and y coordinates, being the bottom phase in the x

axis, and the top phase in the *y* axis. All the systems that share the same tie line length (TLL) have the same physicochemical properties, and as well the same concentration of each component. A TLL (Eq. 1) is constructed by cutting the binodal curve in two points, which represent the composition of each phase, each TLL is at a specific distance from the critic point, just above this point the volume of both phases is theoretically equal. The systems that share the same TLL have different volumes of phase (Fig. 1). This occurs because there is a different solvent (water) migration between both phases. In this way, we can manage the relation between volume of both phase by choosing the global concentration of PEG and phosphate (Asenjo & Andrews, 2011).

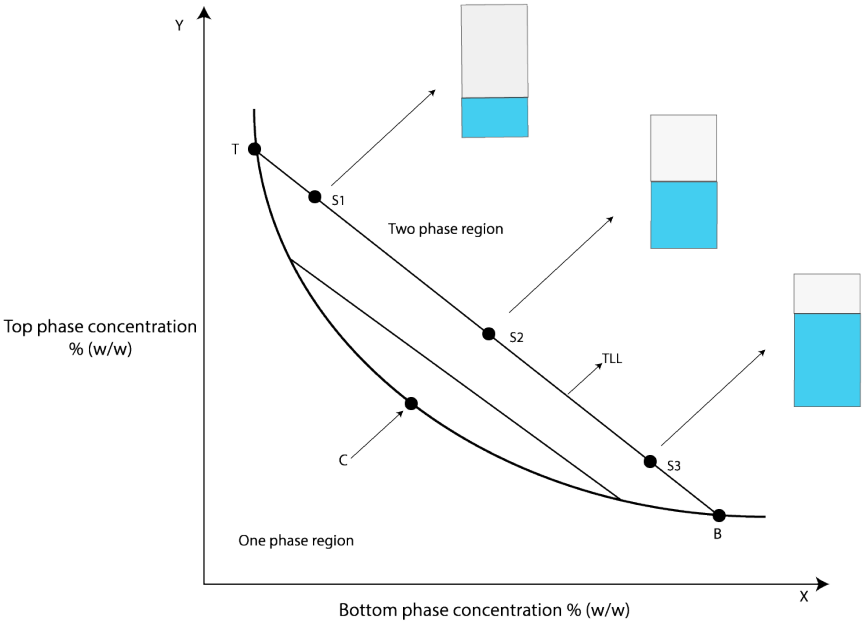

Fig. 1 Binodal diagram in which we find the binodal curve that represents the limits in which the two-phases are formed. S1, S2, and S3 represents different points with a different global concentration, and different volume ratio of each one, but that share the same TLL, which means an equal concentration of top (T) and bottom phase (B). C is the critic point

$$TLL = \sqrt{(\Delta|PEG|)^2 + (\Delta|Salts|)^2} \quad 1)$$

Droplet generation is caused by fluid instabilities. In passive methods the droplet formation is generated by the introduction of one fluid (disperse) in another fluid (continuous), both immiscible with each other. The three most common modes of droplet formation are squeezing, dripping, and jetting. In the squeezing method, the channel geometry plays a major role, while in the other modes, droplets are formed due to capillary instabilities when interfacial forces seek to minimize their area according to the thermodynamic principle of minimum interfacial energy. Viscosity and inertial forces try to deform the liquid/liquid interface, while the surface tension is the force that resist that deformation. The capillary number (Ca) (Eq. 2) represent the relation between these forces, in which μ is the viscosity, U is the velocity of the fluid, and σ is the Surface tension. A $Ca < 10^{-2}$ results in the squeezing regimen, while a $Ca > 10^{-2}$ results in the dripping regime (Zhu & Wang, 2017).

$$Ca = \frac{\mu U}{\sigma} \quad (2)$$

3. Materials and methods

3.1 Microfluidic chip fabrication

Microfluidic chips were fabricated of PDMS by soft lithography as described elsewhere (Mata-Gómez et al., 2016). The microchannel mask was designed using Autodesk AutoCAD 2020 student version (2019 Autodesk, Mill Valley, CAD, USA) available online. The microfluidic chip is based on a flow-focusing geometry consisting of two inlets (where both phases are introduced) and one outlet. Figure (2) shows a schematic representation of the microfluidic device. Liquids intercept at the cross-junction, where droplets are formed. Master molds were fabricated by photolithography. Epoxy negative photoresist polymer SU-8 2100 was coated on a clean glass surface (50 x 50 mm) using a spin coater WS-650 HZB-23NPP/UD3 (Laurell Technologies Corporation, North Wales, PA, USA). The spinning parameters were determined based on the recommendation of the polymer supplier to obtain a final thickness of 100 µm. Afterwards, the polymer was placed on a hot plate at 95 ºC for 25 min, and then left for about 5 minutes at room temperature untiled it cooled down. The photomask was placed over the photoresist and exposed to UV light for 25 seconds using a DYMAX lamp 2000-ECE (INFO), and subsequently heated at 95 ºC for 10 min. The mold was developed for 10 minutes using the developer solution and dried with compressed air. Finally, the master mold was heated at 150 ºC for 10 min. The replica was fabricated by pouring a 10:1 previously degassed mixture of silicon elastomer and curing agent (Sigma Aldrich, 761036) over the master mold, and cured at 120 ºC during 10 min. The inlets of the micro channels were made by using a 2-mm diameter core puncher. Finally, sealing of the device was performed by bonding the PDMS devices to a glass slide (1x3") using an air plasma cleaner (Harrick Plasma, PDC-001, Ithaca, NY, USA), leaving both, replica and glass slide to be exposed to bright pink plasma for 3 minutes.

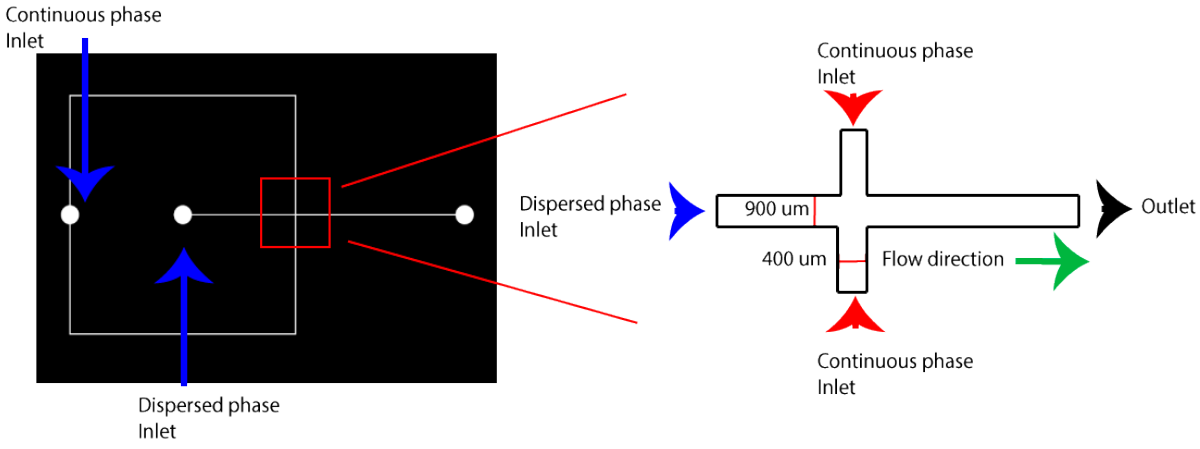

Fig. 2 Representation of microfluidic chip, which is based on a flow focusing device. A continuous phase inlet and a disperse inlet are observed. The cross-shape design allows liquids to meet at the intersection of both continuous and disperse channels, in which droplet formation can occur

3.2 Protein preparation.

Ribonuclease A (RNase A) from bovine pancreas (cat. no. R500, Sigma-Aldrich, San Luis, Missouri, USA) was PEGylated and the mono-PEGylated conjugate was recovered according to chromatographic methodologies previously developed by our group (Mayolo-Deloisa et al., 2012). Native and mono-PEG RNase A were labeled with FITC (cat. no. 46950, Sigma-Aldrich, San Luis, Missouri, USA). Briefly, 684 µl of FITC solution (10 mg/mL) prepared in DMSO, were added to 1200 µL (10 mg/mL) of native or mono-PEG RNase A, which were previously dissolved in 100 mM carbonate buffer at pH 9. The reaction was carried out at room temperature for 1h at constant agitation. Vials with the reaction mixture were covered with aluminum foil to avoid FITC photobleaching. Afterwards, the reaction mixture was adjusted to 2.5 mL, and passed through a 0.22-micron syringe filter. Finally, the sample was loaded into a PD10 column to remove unbound FITC. Microfiltered distilled water was used as eluting solvent. The protein solutions eluted from the PD10 columns were stored at -20 ºC for the following studies.

3.3 Preparation of PEG/Salt ATPS and experimental setup.

PEG-potassium phosphate ATPS were constructed to study the droplet formation phenomenon and its potential in protein fractionation inside the microdevice. A stock solution (50% w/w) of PEG of nominal molecular weight of 8000 g/mol (cat no. 1546605, Sigma-Aldrich, San Luis, Missouri, USA), and dipotassium hydrogen orthophosphate/potassium di-hydrogen orthophosphate (K_2HPO_4 and KH_2PO_4) (18:7, 40% w/w, pH 7) solutions were prepared. ATPS were constructed based on studies conducted before (González-Valdez, Cueto, et al., 2011). Systems with 25% w/w of TLL, 13.0% w/w of PEG, 10.4% w/w of phosphates, 10% w/w of protein sample solution (10 mg/mL), and the rest of water, were constructed. These systems were chosen based on the partition coefficient of both native and mono-PEG RNase A as previously reported by other studies in our group (González-Valdez, Rito-Palomares, et al., 2011).

Four experimental scenarios were performed to evaluate weather native and PEGylated RNase A remained in one phase or were displaced to another phase according to their affinity. In our first experiment, PEG + PEGylated RNase A was chosen as the continuous phase and the phosphate salt solution with no protein was selected as the disperse phase (Fig. 3a). Before loading the device, 10 g systems, constructed as previously mentioned, were prepared in 15 mL tubes and left to rest until the system equilibrated—i.e., when the phases have formed and an interface between them can be seen. Once the phases were formed, they were individually recovered and introduced into the device as presented in Fig. 3a. For the second experimental scenario, PEG and phosphate salt phases were chosen again as continuous and disperse phases, respectively, and native RNase A was added to the salt phase (Fig 3b). Preparation of systems and loading of phases into the device was performed in the same way as for the first scenario. Details of the experimental set-up and how proteins, native or PEGylated, were loaded into the microfluidic device, are described in Fig. 3a, and Fig 3b.

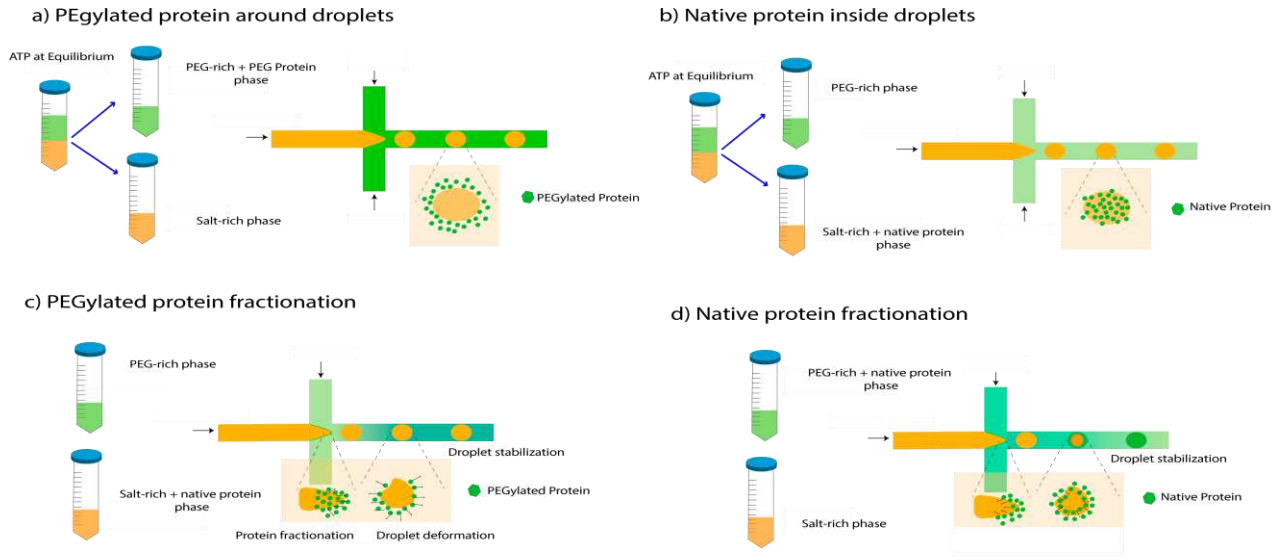

Fig. 3 Illustration of the four different scenarios, and representation of each phase and how they meet at the junction of the channels of the microfluidic devices. a) First experiment in which PEG acts as the continuous phase and phosphate salts as the disperse phase. PEGylated RNase A is introduced within the PEG phase and it is expected to remain there as the salt rich-droplet moves. Both phases were introduced to the microfluidic flow-focusing devices to see droplet formation. b) Illustration of the second experiment. Salt + Native protein are the disperse phase, while PEG is in the continuous phase. Droplet formation with protein encapsulation is expected to occur. Both phases were introduced to the microfluidic flow-focusing devices to see droplet formation. c) Illustration of the third experiment. PEGylated protein is initially in the salt phase to observe its movement towards the PEG phase. When droplet formation occurs, protein fractioning at the interface and deformation of the droplet is expected, with an eventual droplet stabilization. d) Illustration of the fourth experiment. Native protein is initially in the PEG phase to observe its movement to the salt phase. It is expected that native protein causes droplet deformation, but at the same time protein encapsulation

To visualize if the protein (native or PEGylated) shifted from one phase to another, the protein was introduced in the phase for which it has less affinity. So, contrary to the first experiment, in this third scenario, the PEGylated protein was placed in the salt-rich phase to observe protein migration from that phase towards the PEG-rich phase. To properly do this, the ATPS was not previously prepared in a tube as in the two previous experiments. Instead, quantities of both PEG and phosphate salt solution were weighted to reach a TLL of 25% w/w. Ten-gram systems, containing 2.6 g of each phase-forming chemical (PEG and Salt), 3.8 g of water, and 1 g of protein solution, were prepared. The PEG and salt solution was then placed in two different tubes. The PEGylated protein sample was placed inside the salt phase together with 1.4 g of water, while 2.4 g of water were added to the PEG phase. Thus, the salt + PEGylated protein was solubilized in the disperse phase, while the PEG was present in the continuous phase (Fig. 3c). In the same way, for the fourth experimental setup, native protein was placed on the PEG-rich phase to observe its displacement towards the salt-rich phase (Fig. 3d). To do this, we followed the same procedure as in the previous experiment, but in this case, the native protein was placed in the PEG-rich phase to see if it migrated towards the salt-rich phase. For all experiments, flow rate was varied between 7 and 0.07 µL/min, to determine the velocity for droplet formation, using a syringe pump from Chemyx Inc (Model: Fusion 200). As the first scenario consist of an ATPS previously formed and with their properties previously reported, we decided to realized simulations in COMSOL Multiphysics 5.3a using a methodology previously described by us (Hernández-Cid et al., 2020). To do this we take the same geometry a shown in Fig. (3) and we set the fluid properties according to our ATPS, in which the viscosity was set to 8.9 mPa s (González-Tello et al., 1994) and the interfacial tension to 0.012 mN/m at 293 K with a pH of 7 (de Oliveira et al., 2012; Kim & Rha, 2000).

4. Results and discussion

4.1 Droplet formation in PEG/Salt ATPS

Fig. 4 shows the droplet formation of PEG/Salt ATPS for the first experiment, where three different scenarios can be observed. First, the PEG phase with the PEGylated protein enters the continuous channel (transversal channel), while the salt phase enters the disperse phase (main channel). In this case, laminar two-phase flow with defined streamlines of both phases is observed (Fig. 4a), with the salt phase in the middle streamline (dark streamline due to the absence of fluorescence), and the green-fluorescent streamline being the PEG phase with the solubilized PEGylated protein. The system was formed by controlling inertial forces; this is, by changing the velocity of the fluids. The velocity of each phase was increased approximately to a flow rate of 7 µl/min, and values above this showed similar trends in the formation of streamlines. As expected, the PEGylated RNase A remained in the PEG phase as it happens in conventional ATPS systems.

In the second scenario, droplets were formed because of the balance between inertial forces, viscosity (μ) and velocity (U), and surface tension (σ), that is, the capillary number (Eq. 2) In this part, we reduced the flow rate value from 7 µl/min to ~0.7 µl/min. When the system was set to 0.7 µl/min, droplets started to form near the junction (Fig. 4b). As time passed, plug flow, observed from the elongated droplets, started to appear replacing the droplet formation (Fig. 4c). We attributed this to the change of the relation between inertial and surface forces, in which inertial forces decreased as the velocity decreased, giving the opportunity to generate a droplet by the effect of the surface tension. Besides, the effect that the continuous phase pressure exerts on the dispersed phase had an impact, as the former decreased. Overall, it is seen that most of the fluorescence remains on the PEG stream, which indicates the affinity of the PEGylated protein for the PEG rich phase, as in conventional ATPS.

The approximate value of droplet length obtained with the COMSOL simulations was of 220 µm (Fig. 4d), which is comparable to that obtained experimentally, which was 270 µm. This little difference can be attributed to the values of viscosity of the PEG phase, as well as to the value of surface tension that the protein could have changed as observed elsewhere (KITABATAKE & DOI, 1988). Further studies must be done to analyze the effect of the protein on these two liquid properties; however, our simulation provided a good approximation to the experimental observation.

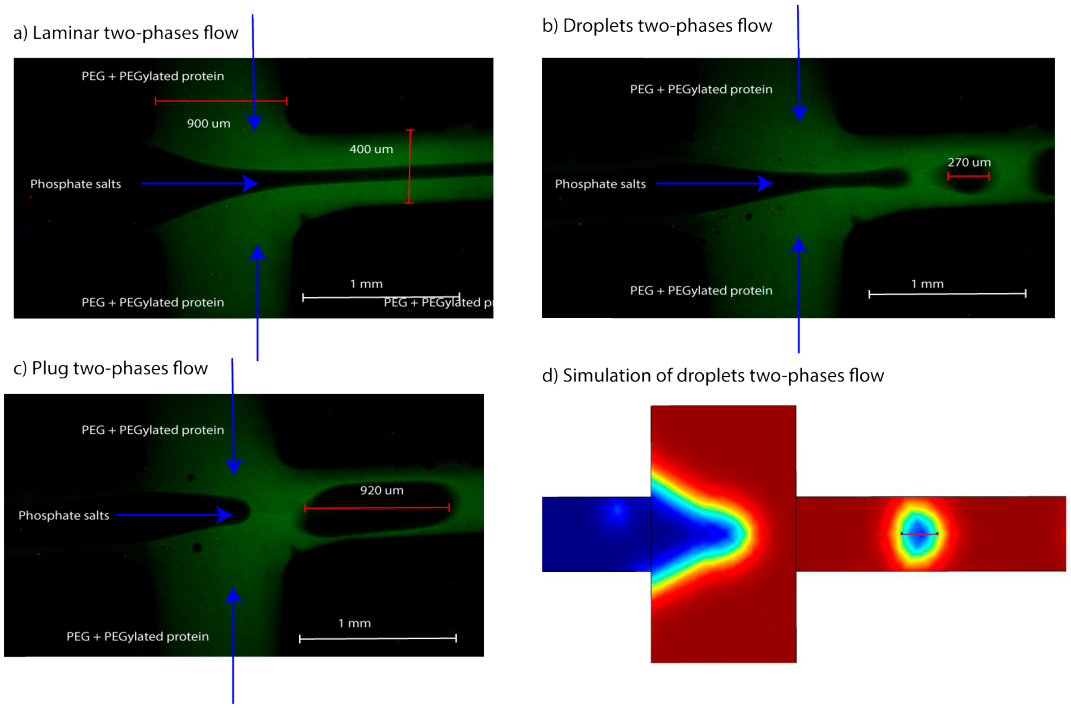

Fig. 4 Micrographs showing how FITC-PEGylated ribonuclease A remains in the PEG-rich phase. (a) Two-phases streamlines, where green zones represent PEG + PEGylated protein phase, while dark zones represent salts phase, (b) droplet formation of salt phase disperse in the continuous PEG phase, (c) plug flow formation of the salt phase, (d) Simulation of ATPS droplets formation

In the second experiment, the salt-rich phase containing native protein was used as the disperse phase (main channel), while PEG-rich phase was used as continuous phase (cross channel). Droplet formation did not occur at the junction of the continuous and disperse channel, instead, two phases flow was formed first (Fig. 5a), and the droplet formation occurred upstream in the main channel (Fig 5b). The fact that droplets did not form is a result of the increasing viscous forces (i.e., the presence of proteins might increase viscosity as some studies have concluded (Gonçalves et al., 2016)). The increase of viscosity had an impact on the capillary number (Eq. 2), which increases, overcoming surface forces, corresponding to the dripping regime ($Ca > 0.1$). Streamlines of the salt phase that come from the disperse channel and stretch upstream in the continuous channel are observed. To overcome this, velocity control can be an option to balance the inertial and viscous forces. In fact, droplet formation did occur when the velocity was slowed down until it reached a flow rate value of 0.07 µl/min. Under this operation condition, monodisperse droplets with a higher frequency were observed to form downstream of the cross section, which is known as the jetting regimen. This regime is generally characterized by an increment of viscous forces over surface forces ($Ca > 10^{-2}$ corresponding to a dripping regime) but in this case as some authors have reported jetting regime can occurs when there is a high contrast of viscosity ratio or flow ratio of both continuous and disperse phase [11, 22]. The approximate value of droplet length obtained was of 180 µm in this experiment. It is also important to observe that the fluorescence of the FITC linked to protein was photobleached, this could be attributed to the phosphate salts, as it has been found that high concentrations of them influence absorption, quenching FITC fluorescence (Sharma Biomed Sci & Res, n.d.; Struganova et al., 2002).

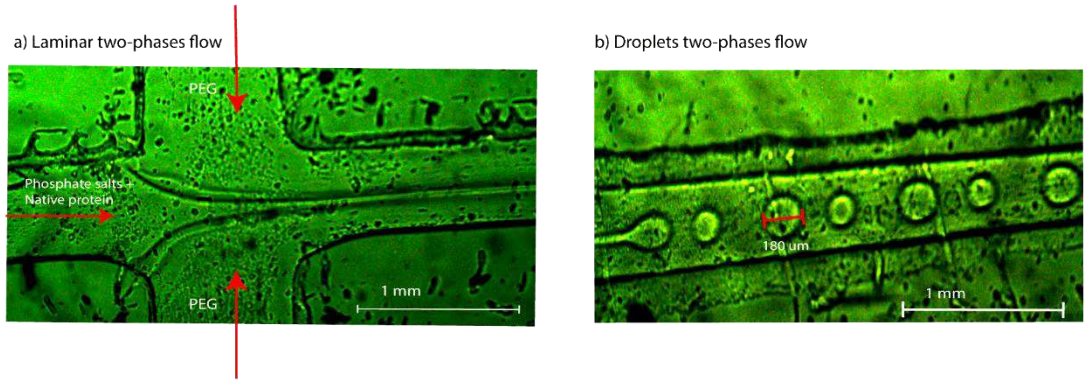

Fig. 5 Images showing how FITC-native ribonuclease A remains in the salt-rich phase. (a) Droplet formation of salt + protein phase downstream in the channel after the streamline get disrupted and (b) streamlines formation of the two-phase PEG and Salt + Protein

4.2 Protein partition between phases

The third experiment tested how PEGylated protein molecules displace outside the salt phase into the PEG phase. In this scenario (Fig. 6), when droplet formation was achieved, three main stages were identified: 1) protein partition at the interface between both liquids before droplet formation, 2) droplet formation, in which droplets are deformed, apparently due to protein migration from the salt-rich phase to the rich-PEG phase, and 3) an apparent droplet stabilization. Droplet length value obtained here was of approximately 370 µm. Presumably, due to the displacement of proteins from one phase to another, the formation of microdroplets was affected, which is observed in the monodispersivity.

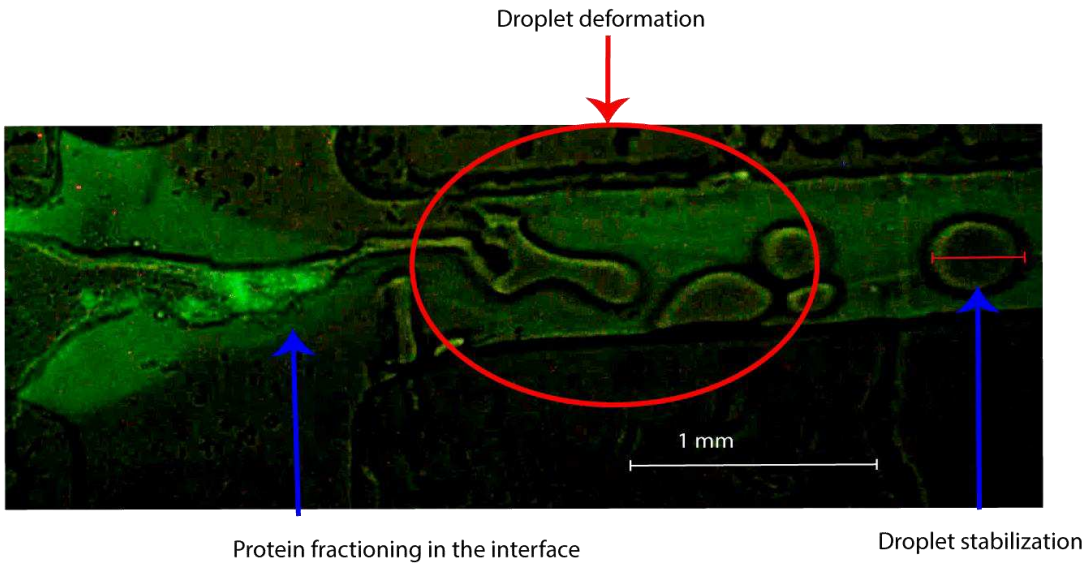

Fig. 6 PEGylated ribonuclease A partitioning from the salt phase to the PEG-rich phase and droplet formation. It is clearly seen that protein is displacing form the salt phase to the PEG phase when droplet formation occurs. Later, the droplet suffers a deformation due to protein displacement, and is finally stabilized

When introducing PEGylated RNase A in the salt-rich phase to study its partition behavior towards the PEG-phase (Fig. 7a), a two-phase flow streamline was achieved. In these streamlines, the outer phases correspond to the PEG-phase, while the non-fluorescent stream in the center represents the salt-rich phase. This stream-like pattern occurs when inertial forces are higher as compared to surface forces, which in turn is traduced in a high velocity ($Ca > 1$); here, it occurred at a flowrate of 7 µl/min. In this scenario, it was seen how protein started to migrate from one phase to the other starting at the interface, *i.e.* the contact region between both phases. This can be observed either in the intersection of the channel (Fig. 7a) or downstream (Fig. 7b). As both phases move downstream, a major fluorescence in the PEG phase is clearly seen, which corresponds to the outer streamlines, while the streamline in the middle, the salt phase, has lost part of the visible fluorescence that it presented at the beginning, indicating that protein moved to the higher affinity phase as hypothesized.

On the other hand, lowering the flow velocity favored the formation of droplets. Likewise, the partition of the PEGylated protein from the salt rich-phase to the PEG phase was observed at the interface (Fig. 7c). However, as the droplet forms, at the cross-section area, it can be observed how most fluoresce remains outside the droplets (Fig. 7d). Before this occurs, droplets suffer deformation, which presumable could be attributed to the protein movement from the salt-rich phase to the PEG-rich phase, trespassing and deforming the interface that eventually stabilizes generating droplets of uniform shape, in which most of the fluorescent protein molecules have made their way outside the droplet as suggested by the near absence of fluorescence.

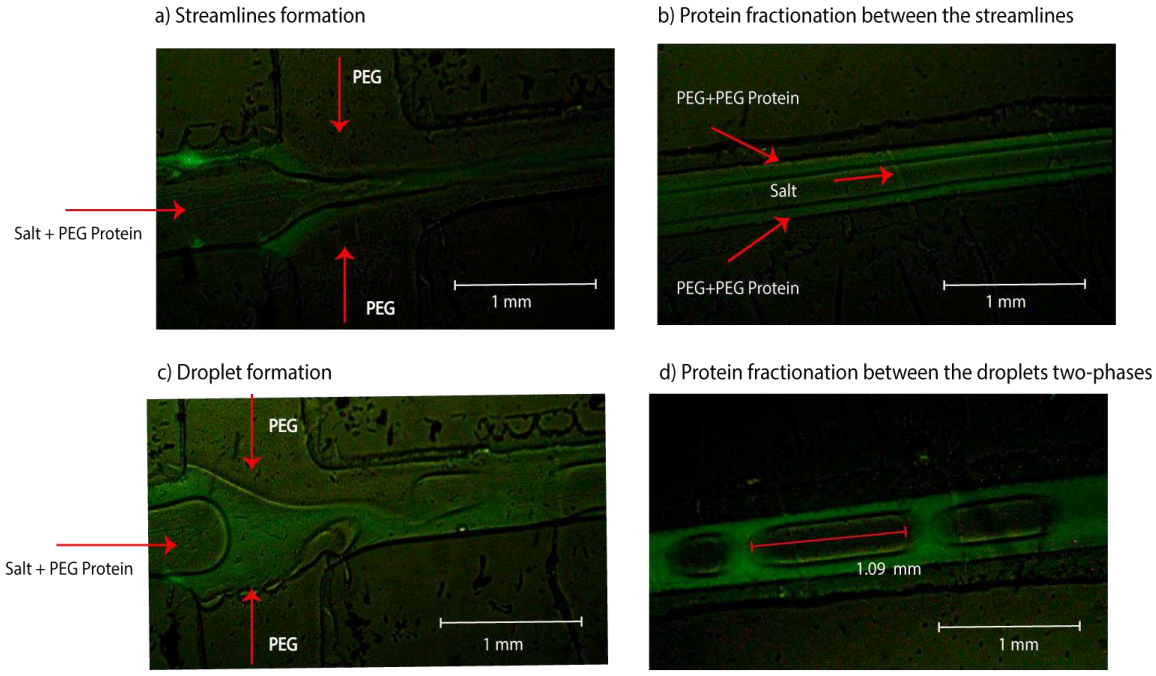

Fig. 7 (a)Partition of FITC-PEGylated ribonuclease A inside the ATPS droplet microfluidic system. Images show partition of protein from salt rich phase to PEG-rich phase either when two phases are formed (a and b) or when droplets were formed (c and d). Flow goes from left to right. In this scenario, PEGylated protein was introduced in the sal-rich phase

In the fourth experiment, native FITC-labeled RNase A was introduced into the device by the inlet carrying the PEG-rich phase, that is, the continuous phase. A two-phase streamline was produced again as shown in Fig.

(8). It is observed how proteins disrupted the salt streamline due to the protein partition from PEG rich-phase to the salt-rich phase. This happened because inertial forces overcame surface tension ($Ca > 1$). In this experiment, three stages were identified. 1) The salt streamline forms (Fig. 8a), followed by 2) a displacement of protein from the PEG phase to the salt phase (Fig. 8b), which caused a discontinuity of the salt phase, and finally 3) a total disruption of the phase, in which protein has already disrupted the salt-rich phase (Fig. 8c). Unlike the other experiments, in this experiment we can highlight that the streamlines were formed followed by their disruption, this can be attribute to the move of the protein from PEG phase (less affinity) to the salt phase (more affinity). We were able to observe a kind of curvature in the streamline (Fig. 8a), which we attributed to the effect of protein displacement from one phase to the other. Experiments for droplet formation were also carried out when studying migration of native protein towards the salt-rich phase. To produce droplets, the flow rate was lowered 10 times, approximately 0.7 µl/min. In this scenario, it was found that three different stages occurred as shown in Fig. (8). In the same way as the previously analyzed scenarios, droplet formation started to occur at the interface. 1) A dispersion of the salt phase in the PEG phase by an apparently droplet detachment is observed. 2) Here, it was found that the protein enters to the droplet since the moment of detachment (Fig. 8d), which in the second stage resulted in an incomplete droplet formation and salt phase deformation (Fig. 8e). And finally, 3) a reshape of the salt droplets with fluorescent protein encapsulation was observed. Although, this is not always the case, since usually the salt phase mix with the other phase (Fig. 8f). This can be attributed to the higher protein concentration in the medium, as well as to the change in the surface tension of the salt phase because the presence of protein inside that phase. In fact, when exceeding the capacity of conventional ATPS systems interphase is disrupted given rise to a single-phase system. Further studies and approaches need to be explored to achieve droplet stabilization and protein encapsulation. This can be done by modifying surface tension using chemicals or other forces as electrical force (Zhu & Wang, 2017). Overall, we see how native protein tends to move from the PEG phase towards the salt phase, in which droplets suffer a complete disruption because protein displacement in most of the cases. These results suggest a further implementation of this technology for the fractionation of protein depending on their phase affinity.

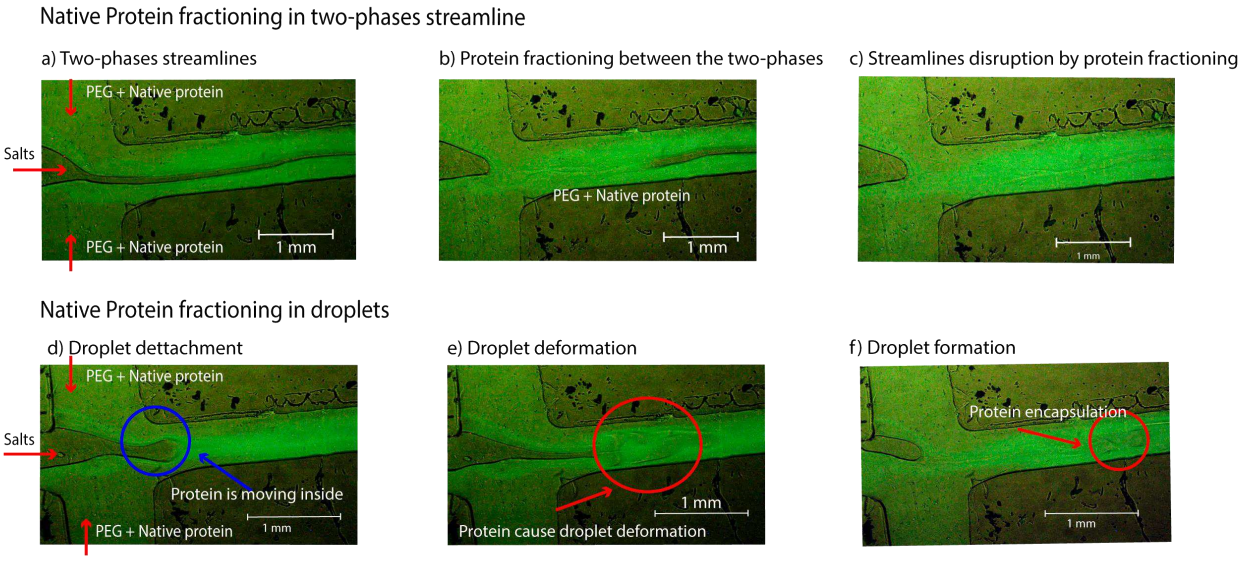

Fig. 8 Images visualizing partition behavior of native FITC-ribonuclease A inside the device. First, a) a two-phases streamline was generated, later b) native protein started to move from PEG phase to the salt streamlines, which cause a c) disruption of the salt phase, and finally a complete disruption of the salt phase streamline due to the movement of native protein to the salt phase. Illustration of the process of droplet formation, and protein movement when studying native RNase A partition. d) In the first stage we see how protein is entering into the droplet, later e) that protein movement cause a protein deformation which can lead to an eventually f) droplet stabilization, and therefore protein encapsulation

5. Conclusions

Protein partition and separation in microfluidic devices has the potential to become a powerful tool to carry out downstream microbioprocess. In our work, we tested how model proteins, native and PEGylated RNase A, fractionate in a microfluidic system using droplet-based aqueous two-phases systems (ATPS). So far, we have found that even when there is a moving fluid, in which one of the two phases have discontinuities such as droplets, model proteins partition to their preferred phase, as they do in conventional ATPS systems. With this approach, we have visualized several phenomena. 1) Streamlines and droplet formations of ATPS with both native and PEGylated proteins. 2) Protein displacement form one phase to the other phase in both streamlines and droplet systems. 3) Protein disruption of streamlines and droplet. So far, we have been able to demonstrate that proteins behave in the same manner as they do in conventional ATPS systems regardless of whether droplets form or not. These results open new opportunities for future developments and quantitative characterization of these phenomena (diffusion and convection), or to calculate protein yield in each phase for protein recuperation.

Overall, this first approach can be a part of a total process on a chip. For example, the disperse phase can be the products of a reaction, in which the undesired products can be separated to the other phase according to their affinity, or even droplets acting as microreactors that separate undesired residues at the same time. Today, there are few reports, which work using PEG and salt systems inside a microfluidic device, and even less attempts to implement this for the separation of proteins. For instance, this first approach allowed the visualization of how model proteins behave in the device. Nonetheless, this field needs more attention before implementing this technology in the design of microfluidic platforms dedicated to performing microbioprocesses in an efficient manner.

Acknowledgments

Authors thank Tecnologico de Monterrey for the technological platform and CONACyT for supporting David Hernández Cid through the grant No. 732347.

Declarations

Funding

This project was financed by the Tecnologico de Monterrey through the Bioprocess Research Group and the Sensors and Devices Research Group.

Conflict of interst

The authors have no conflicts of interest to declare that are relevant to the content of this article.

Availability of data and material (data transparency)

Not applicable

Code availability (software application or custom code)

Not applicable

Author contributions

Not applicable

Additional declarations for articles in life science journals that report the results of studies involving humans and/or animals

Ethics approval (include appropriate approvals or waivers)

Not applicable

Consent to participate (include appropriate statements)

Not applicable

Consent for publication (include appropriate statements)

Not applicable

References

Asenjo, J. A., & Andrews, B. A. (2011). Aqueous two-phase systems for protein separation: A perspective. In *Journal of Chromatography A* (Vol. 1218, Issue 49, pp. 8826–8835). Elsevier. https://doi.org/10.1016/j.chroma.2011.06.051

de Oliveira, C. C., Coimbra, J. S. D. R., Zuniga, A. D. G., Martins, J. P., & Siqueira, A. M. D. O. (2012). Interfacial tension of aqueous two-phase systems containing poly(ethylene glycol) and potassium phosphate. *Journal of Chemical and Engineering Data*, *57*(6), 1648–1652. https://doi.org/10.1021/je1010104

Gonçalves, A. D., Alexander, C., Roberts, C. J., Spain, S. G., Uddin, S., & Allen, S. (2016). The effect of protein concentration on the viscosity of a recombinant albumin solution formulation. *RSC Advances*, *6*(18), 15143–15154. https://doi.org/10.1039/c5ra21068b

González-Tello, P., Camacho, F., & Blázquez, G. (1994). Density and Viscosity of Concentrated Aqueous Solutions of Polyethylene Glycol. *Journal of Chemical and Engineering Data*, *39*(3), 611–614. https://doi.org/10.1021/je00015a050

González-Valdez, J., Cueto, L. F., Benavides, J., & Rito-Palomares, M. (2011). Potential application of aqueous two-phase systems for the fractionation of RNase A and α-Lactalbumin from their PEGylated conjugates. *Journal of Chemical Technology & Biotechnology*, *86*(1), 26–33. https://doi.org/10.1002/jctb.2507

González-Valdez, J., Rito-Palomares, M., & Benavides, J. (2011). Quantification of RNase A and Its PEGylated Conjugates on Polymer-Salt Rich Environments Using UV Spectrophotometry. *Analytical Letters*, *44*(5), 800–814. https://doi.org/10.1080/00032711003789959

Hardt, S., & Hahn, T. (2012). Microfluidics with aqueous two-phase systems. *Lab Chip*, *12*(3), 434–442. https://doi.org/10.1039/C1LC20569B

Hatti-Kaul, R. (2001). Aqueous two-phase systems: A general overview. In *Applied Biochemistry and Biotechnology - Part B Molecular Biotechnology* (Vol. 19, Issue 3, pp. 269–277). Springer. https://doi.org/10.1385/MB:19:3:269

Hernández-Cid, D., Pérez-González, V. H., Gallo-Villanueva, R. C., González-Valdez, J., & Mata-Gómez, M. A. (2020). Modeling droplet formation in microfluidic flow-focusing devices using the two-phases level set method. *Materials Today: Proceedings*. https://doi.org/10.1016/j.matpr.2020.09.417

Kim, C. W., & Rha, C. (2000). Interfacial tension of polyethylene glycol/potassium phosphate aqueous two-phase systems. *Physics and Chemistry of Liquids*, *38*(1), 25–34. https://doi.org/10.1080/00319100008045294

KITABATAKE, N., & DOI, E. (1988). Surface Tension and Foamability of Protein and Surfactant Solutions. *Journal of Food Science*, *53*(5), 1542–1569. https://doi.org/10.1111/J.1365-2621.1988.TB09319.X

Lu, Y., Xia, Y., & Luo, G. (2011). Phase separation of parallel laminar flow for aqueous two phase systems in branched microchannel. *Microfluidics and Nanofluidics*, *10*(5), 1079–1086. https://doi.org/10.1007/s10404-010-0736-7

Mastiani, M., Firoozi, N., Petrozzi, N., Seo, S., & Kim, M. (2019). Polymer-Salt Aqueous Two-Phase System (ATPS) Micro-Droplets for Cell Encapsulation. *Scientific Reports*, *9*(1), 15561. https://doi.org/10.1038/s41598-019-51958-4

Mata-Gómez, M. A., Gallo-Villanueva, R. C., González-Valdez, J., Martínez-Chapa, S. O., & Rito-Palomares, M. (2016). Dielectrophoretic behavior of PEGylated RNase A inside a microchannel with diamond-shaped insulating posts. *Electrophoresis*, *37*(3), 519–528. https://doi.org/10.1002/elps.201500311

Mayolo-Deloisa, K., Lienqueo, M. E., Andrews, B., Rito-Palomares, M., & Asenjo, J. A. (2012). Hydrophobic interaction chromatography for purification of monoPEGylated RNase A. *Journal of Chromatography A*, *1242*, 11–16. https://doi.org/10.1016/j.chroma.2012.03.079

Meagher, R. J., Light, Y. K., & Singh, A. K. (2008). Rapid, continuous purification of proteins in a microfluidic device using genetically-engineered partition tags. *Lab on a Chip*, *8*(4), 527–532. https://doi.org/10.1039/b716462a

Moon, B.-U., Jones, S. G., Hwang, D. K., & Tsai, S. S. H. (2015). Microfluidic generation of aqueous two-phase system (ATPS) droplets by controlled pulsating inlet pressures. *Lab on a Chip*, *15*(11), 2437–2444. https://doi.org/10.1039/C5LC00217F

Sharma Biomed Sci, A. J., & Res, T. (n.d.). *Evaluation of Various Factors Affecting Fluorescence Emission Behavior of Ochratoxin A: Effect of pH, Solvent and Salt Composition*. https://doi.org/10.26717/BJSTR.2018.10.001979

Song, H., Chen, D. L., & Ismagilov, R. F. (2006). Reactions in Droplets in Microfluidic Channels. *Angewandte Chemie International Edition*, *45*(44), 7336–7356. https://doi.org/10.1002/anie.200601554

Struganova, I. A., Lim, H., & Morgan, S. A. (2002). The influence of inorganic salts and bases on the formation of the J-band in the absorption and fluorescence spectra of the diluted aqueous solutions of TDBC. *Journal of Physical Chemistry B*, *106*(42), 11047–11050. https://doi.org/10.1021/jp013511w

493 Taly, V., Kelly, B. T., & Griffiths, A. D. (2007). Droplets as Microreactors for High-Throughput Biology.
494 *ChemBioChem*, *8*(3), 263–272. https://doi.org/10.1002/CBIC.200600425

495 Zhou, C., Zhu, P., Tian, Y., Tang, X., Shi, R., & Wang, L. (2017). Microfluidic generation of aqueous two-
496 phase-system (ATPS) droplets by oil-droplet choppers. *Lab on a Chip*, *17*(19), 3310–3317.
497 https://doi.org/10.1039/C7LC00696A

498 Zhu, P., & Wang, L. (2017). Passive and active droplet generation with microfluidics: a review. *Lab on a*
499 *Chip*, *17*(1), 34–75. https://doi.org/10.1039/C6LC01018K

500

501